Effect of Vibration on the Heat Transfer Process in the Developing Region of Annulus with Rotating Inner Cylinder

Dr. Mauwafak A. Tawfik
Mechanical Engineering Department, University of Technology/ Baghdad.
Dr. Akeel A. Mohammed
Petroleum Technology Department, University of Technology/ Baghdad .
Hayder Zuhair Zain
Mechanical Engineering Department, University of Cufa/Al Najaf.
Email:h.zainy@yahoo.com

Received on:6/12/2012 & Accepted on:29/1/2015

ABSTRACT

Experimental investigation has been carried out to study the effect of induced vibration on the heat transfer process in the simultaneously developing of hydrodynamic and thermal boundary layer region of a concentric vertical annulus with uniformly heated outer cylinder and rotating solid inner cylinder. The experimental setup consists of an annulus, which has a radius ratio of 0.365 and outer cylinder with a heated length 1.2 m subjected to the constant heat flux. The investigation covers Reynolds number (Re) range from 514 to 1991, Taylor number (Ta) values are 10.44×10^4 & 82.23×10^4, heat flux varied from 468 W/m^2 to 920 W/m^2 and frequency (Fr) values are 32 & 77 Hz. Results showed for all frequency values that the local Nusselt number values increase as the heat flux increases when the value of frequency near the natural frequency and the value of the surface radiation decrease. Correlation equations have been deduced to calculate the rate of heat transfer, represented by the average Nusselt number (Nu_m) as a function of (Ta), (Ra) and (Fr). A comparison has been made between the present work and the previous works for temperature and local Nusselt number variations and it has given a good agreement.

Keywords: Heat transfer, Annulus, Rotating Inner Cylinder, Vibration.

تأثير الاهتزاز على عملية انتقال الحرارة بمنطقة التشكيل لتجويف حلقي باسطوانة داخلية دوارة

الخلاصة:

أجريت دراسة عملية لأيجاد تأثير الأهتزاز على عمليات انتقال الحرارة الموقعي و المعدل بالحمل المختلط لجريان الهواء المشكل تراكبياً (اي تزامن التشكيل الحراري مع التشكيل الهيدروديناميكي) بتجويف حلقي بين اسطوانتين متحدتي المركز، حيث ان الاسطوانة الخارجية مثبتة الطرفين و مسلط عليها اهتزاز قسري. سخنت الاسطوانة الخارجية تحت فيض حراري ثابت و الاسطوانة الداخلية دوارة نسبة نصف القطر لهما تعادل 0.365 و أسطوانة خارجية بطول 1.2 م معرضة الى فيض حراري منتظم . يتراوح معدل رقم Re في هذا البحث من

514 الى 1991 أما الفيض الحراري فيتغير من 468 W/m^2 الى 920 W/m^2 ، و مقدار الاهتزاز القسري Fr هو 32 & 77 Hz وقيمتي رقم Ta هما 82.23×10^4 & 10.44×10^4.

بينت النتائج العملية ان قيم رقم Nu تزداد بزيادة الفيض الحراري و بوجود الاهتزاز حسب اقتراب التردد من التردد الطبيعي. تم ايجاد معادلات تجريبية لحساب معدل رقم Nu كدالة مع رقم Ta و رقم Ra و مقدار الاهتزاز Fr . أجريت مقارنة لتغير رقم Nu الموقعي و درجة الحرارة مع الطول اللابعدي للاسطوانة الداخلية للبحث الحالي مع بحوث سابقة و أعطت قبول جيد.

INTRODUCTION

Generally, more studies concerned with the effect of vibration on heat transfer can be classified into two types that the heat transfer surface is experimentally vibrated and sub divided into two methods. In the first method, the surface is held stationary, and vibrations are established in the fluid medium surrounding the surface. In the second method, an oscillatory motion is supplied upon the surface itself [1]. Both mechanical and acoustical vibrations have the same phenomenon; each creates an oscillating relative velocity vector between a fluid and the heated surface. The studies in this field can be used either to increase the heat transfer rates in industrial units or to avoid the over-design of heat transfer elements subjected to induced vibration. Most previous studies, however, have dealt with only natural convection heat transfer with mechanical or acoustical vibration. The importance of vibrational motion of the heated surface is to increase the eddies of the flow around the heated surface and may increase the heat transfer coefficient. The intensity of vibration represents a control parameter in the vibrational motion. It depends on both the amplitude (A) and frequency (Fr) and the product of these two parameters. The applications include rotating electric motor, chemical mixing process, swirl nozzles, combustion chambers, fiber coating applications and drying machinery, gas or oil exploration drills, journal bearing, rotating heat exchangers, atmospheric circulation, cooling of rotor blades of gas-turbines, ramjets attached to the rotors of helicopters and rotating condensers for sea water distillation [2].

Many researchers studied experimentally the effect of vibration on the heat transfer. ***Anantanarayanan and Ramachandran*** (1958) , [3] observed an increase of (130) percent in the heat transfer from a vibrating horizontal nichrome wire, (0.018 in) in diameter to an air stream flowing parallel to the wire. The wire was vibrated in a vertical plane with varying values of vibration velocity. The ratio of the vibrational velocity to the flow velocity used in their study varied from (0) to (30) percent. ***Lemlich*** (1961) , [4] published two interesting studies of the effect of vibration on the forced convection heat transfer in a double pipe heat exchanger. In one study, a clarinet mouthpiece placed on the center tube was used to obtain air vibration of about 600 Hz. It is concluded that the average heat transfer was increased by 35 percent with vibration. In a similar study (1961) [5], he used a specially designed pulsator to obtain vibrations of about 1.5 Hz. In this study, the overall heat exchanger efficiency was increased by 80 percent. ***Sreenivasan and Ramachandran*** (1961), [6] investigated the effect of vibration on the heat transfer from a horizontal copper cylinder. The cylinder was placed normal to an air stream and was vibrated in a direction perpendicular to the air stream .The flow velocity varied from (19 ft/s) to (92 ft/s), the double amplitude of vibration from (0.75 cm) to (3.2 cm), and the frequency of vibration from (200 -2800 cycle/min). Results showed that the heat transfer from the cylinder subjected to vibration in a direction perpendicular to the

direction of the air stream remained unaffected when the ratio of the root-mean square velocity of vibration to the flow velocity was varied from 4 to 20 percent. ***Thrasher*** (1967), [7] built much of the equipment used in this investigation. He used photocells to optically record the instantaneous heat transfer by convection from both a 0.003 and 0.008 in. Vibrating wire to still air. The frequency of vibration varied from 20 to 40 Hz and the amplitude from 0.79 to 1.25 in. A (1.5) percent increase in the convective coefficients was observed in the free convection range, but a (20) percent decrease was observed in the forced convection range. The results showed a decrease in heat transfer in the forced convection range. ***Faircloth and Schaaetzle*** (1969), [8] investigated the effect of vibration on the heat transfer for a flow normal to a cylinder. A 40 gauge wires were vibrated in the horizontal plane by a sinusoidal current and simultaneously exposed to a forced air current in the same plane. The frequency and amplitude of the wire varied within the range 20 to 40 Hz and 0.3 to 0.5 in, respectively, Reynolds number experienced by the wire varied between 0 to 15. The results revealed that above a critical Reynolds number, the instantaneous convective coefficient was increased from 20 to 30 percent. ***Kotake and Aoki*** (1984), [9] investigated the unsteady heat transfer of oscillating wake flow, the heat transfer characteristics of a cylinder in wake flows behind a cylinder located in oscillating flows. Their equipment could be provided exactly sinusoidal oscillations flows of velocities from 0 to 60 m/s and the amplitudes of surface temperature, hence the local heat transfer coefficient of the cylinder in oscillating wake flows was roughly proportional to those of the mean flow velocity and inversely proportional to its frequency, although its time-mean was hardly affected by the mean flow oscillation. ***Makki. H. Al-Ubaydi*** (2001), [10] studied the effect of vibration on the heat transfer by free convection using an aluminum cylinder heated at a constant heat flux by passing electrical current through a (Ni-Cr) resistance. The resistance was fixed through the internal space of the cylinder with different angles of slope between (0-45 ^{o}C). It was found that the heat transfer coefficients increased with the increasing of the vibration, but the increasing in heat flux caused decreasing the vibration heat transfer coefficients. ***Lee and Chang*** (2003), [11] investigated the effect of vibration on the critical heat flux (CHF) in a vertical round tube in order to gain an understanding of the relationship between (CHF) and the flow-induced vibration (FIV). The experiment was carried out in the following range of parameters: Diameter D=0.008 m, heated length L=0.2 and 0.4 m, pressure P=101 kPa, Mass flux G=403 to 2551 kg/m^2.s, Amplitude A=0.0001 to 0.001 m, frequency Fr=0 to 70 Hz. The (CHF), generally, increased with vibration intensity which was represented by the vibrational Reynolds number (Re_v); the (CHF) enhancement was more dependent on amplitude than on frequency. ***Dae , et al*** (2007), [12] examined the effects of mechanical vibrations on the critical heat flux (CHF) at atmospheric pressure in a vertical annulus tube under electrically heated condition. Results showed that the vibration of heating rod was increased as the flow regime changed from sub cooled region to bubbly region and the critical heat flux (CHF) was increased by mechanical vibration up to 16.4%. Vibration amplitude was one of the effective parameters on (CHF) enhancement.

The lack in the researches that studied the effect of vibration on the combined convection heat transfer in an annulus in spite of its importance in the industrial applications have been motivated to perform the present work. The aim of the present work is constructing an experimental rig to study the effect of the vibration, Reynolds

number, Taylor number, and heat flux on the mixed convection heat transfer in the entrance region of the annulus with uniformly heated outer cylinder and rotated inner cylinder. In addition to deduce an empirical equation of the average Nusselt number as a function of Re, Ra, and frequency in order to give pronounced insite to the physical behavior of vibration, flow and heat transfer process. The vibration vector was perpendicular to the fluid flow direction with a wide range of Reynolds number (Re =514, 931, 1316, and 1991), Taylor number ($Ta=10.44\times10^4$ & 82.23×10^4) , heat flux (q=468, 642, 920 W/m^2) and excitation frequency of the outer cylinder of the annular (Fr = 32 & 77 Hz).

Experimental Apparatus

The experimental apparatus is shown diagrammatically in Fig.(1). It consists essentially of a cylindrical concentric annulus and the test section as a part of an open air loop, mounted on iron frame (I) which is forced to vibrate (Sh) around a vertical shaft (V). The experimental device is divided into seven main parts as follows: test cylinder section, open air loop, heater circuit, and thermocouple circuit, rotating system, vibration excitation system, and measuring system. The test section consists of 3.5 mm wall thickness, 59.3 mm outside diameter and 1.2 m long aluminum cylinder. The cylinder was electrically heated using a nickel-chromium wire electrical heater. The wire is electrically insulated by means of ceramic beads and is uniformly wound along the cylinder length over an asbestos fiber of (2 mm) thickness in order to give a uniform heat flux. The outside of the test section was then thermally insulated, covered with 60 mm and 5.7 mm as the thickness of the asbestos rope layer and fiber glass, respectively. The cylinder surface temperatures were measured by seventeen asbestos sheath thermocouples (type K), with a temperature range from -200 to 1300°C. The thermocouples were arranged along the outer cylinder and fixed by drilling 17 holes (T) of 2 mm diameter and approximately 3 mm deep in and along the outer cylinder wall, while the ends of the holes chamfered by a drill. Then, the measuring junctions were secured permanently in the holes by a high temperature application epoxy steel adhesive (U). The excess adhesive was removed, and the outer cylinder surface was carefully cleaned with fine grinding paper. All the thermocouple wires and heater terminals were taken out the test section.

An open air circuit was used, which included a centrifugal fan (B), orifice plate section (C), settling chamber (F), and flexible hose (E). The air which is driven by a centrifugal fan can be regulated by using a control valve. The air, induced by the centrifugal fan, enters the orifice pipe section (British Standard Unit) and then settling chamber through a flexible hose (E). The settling chamber was carefully designed to reduce the flow fluctuations and to get a uniform flow at the test section entrance by using flow straightener (G). The air then passed through 1.2 m long test section. A symmetric flow and a uniform velocity profile produced by a well designed teflon bell mouth (H) which was fitted at the beginning of the aluminum cylinder (N) and bolted in the other side inside the settling chamber (F). Another Teflon piece (H) was fitted at the cylinder exit. The teflon was chosen due to its low thermal conductivity to reduce the heat loss from the aluminum cylinder ends. The inlet air temperature was measured by one thermocouple located in the settling chamber (F), while the outlet bulk air temperature was measured by two thermocouples located in the test section exit (R). The local bulk air temperature was calculated by using a straight line interpolation between the measured inlet and outlet bulk air temperature. All

thermocouples were used with leads and calibrated using the melting point of ice made from distilled water as a reference point, the boiling point of distilled water and the boiling points of several pure chemical substances. To determine the heat loss from the test section ends, two thermocouples were fixed in each teflon piece. Knowing the distance between these thermocouples and the thermal conductivity of the teflon, the heat ends loss thus can be calculated.

The block diagram in Fig.(3) shows the instruments used for the vibration test. The air was supplied to the tested modal from a centrifugal fan. Vibration exciter (type 4812 , B&K) is connected, centered to the outer cylinder to excite the modal (test cylinder). The exciter was driven through a power amplifier (type 2712, B&K) by a function generator with autorange counter (60MHz) (type Lutron FG-2003). The response of the modal is picked up by accelerometer (type 4370 B&K) with sensitivity of (4.5 pe/ms^2) fixed by means of screw of ring cap in the middle of the test cylinder. The signal is transmitted to a digital storage oscilloscope (type- Atten ADS 1022C, 500 Msa/s), through the condition amplifier (type 2626 B&K).

Experimental Procedure

To carry out the experiments, the following procedure was followed:

1. The centrifugal fan was switched on to circulate the air, through the open loop. A regulating valve was used for adjusting the required mass flow rate.

2. The inner solid cylinder was rotated by using a belt and variable pulleys diameter and electric motor

3. The electric heater was switched on, and the heater input power was then adjusted to give the required heat flux.

4. The outer cylinder was vibrated by exciter in mid length.

5. The apparatus was left at least three hours to establish a steady-state condition. The thermocouples readings were taken every half an hour by means of the digital electronic thermometer until the reading became constant, a final reading was recorded. The input power to the heater could be increased to cover another run in a shorter period of time and to obtain steady state conditions for next heat flux and same Reynolds number.

6. Run for varying the exciter frequency range of the test cylinder to find its effect on temperatures.

7. During each test run , the following readings were recorded:

a. The reading of the manometer (air flow rate) in mm H_2O.
b. The readings of the thermocouples in ˚C.
c. The heater current in amperes.
d. The heater voltage in volts.

8. Repeat the procedure, but for new values of heat flux, Reynolds number, angular velocity of inner cylinder, and frequency.

Data Analysis

Simplified steps were used to analyze the heat transfer process for the air flow in a cylinder when its surface was subjected to a uniform heat flux.

The total input power supplied to the cylinder can be calculated:

$$Q_t = V'' \times I \qquad \ldots.(1)$$

The convection and radiation heat transferred from the cylinder is :

$Q_{cr}=Q_t-Q_{cond}$ ….(2)

Where
Qcond is the conduction heat loss which was found from the following equation:

$$Q_{cond.} = \frac{\Delta T_{oi}}{\frac{\ln \frac{r_o}{r_i}}{2\pi k_a L}} \quad \text{….(3)}$$

$\Delta T_{oi}=T_o-T_i$
T_o, T_i =average outer and inner lagging surface temperature respectively
r_o=the distance from center of the cylinder to the outer lagging surface
r_i=the distance from center of the cylinder to the beginning lagging (radius of outer cylinder surface)
L=length of cylinder
K_a=thermal conductivity of asbestos=0.161 W/m^3.°C

The convection and radiation heat flux can be represented by:

$q_{cr}=Q_{cr}/A_o$ ….(4)

Where:
$A_o=2\pi r_o L$
A_o =outer surface area of cylinder

The local radiation heat flux can be calculated from the expression [43]:

$$q_r = F_{1-2}\,\varepsilon\,\sigma\left[(T_s)_z + 273\right)^4 - \left(\overline{(T_s)}_z + 273\right)^4\Big] \quad \text{…(5)}$$

Where:
$(T_s)_z$ = local temperature of cylinder.
$\overline{(T_s)}_z$ = average temperature of cylinder.
σ = Stefan beltzman = 5.66×10^{-8} W/m^2 °K^4
ε = emissivity of the polished aluminum surface=0.09.
$F_{1-2}\approx1$
Hence, the convection heat flux at any position is:
$q=q_{cr}-q_r$ ....(6)
The radiation heat flux is very small and can be neglected.
Hence:
$q_{cr}\approx q$ = convection heat flux
The local heat transfer coefficient can be obtained as:

$$h_z = \frac{q}{(T_s)_z - (T_b)_z} \quad \text{….(7)}$$

$(T_b)_z$ = Local bulk air temperature.

All the air properties are evaluated at the mean film air temperature. [14]

$$(T_f)_z = \frac{(T_s)_z + (T_b)_z}{2} \quad \ldots(8)$$

T_f = Local mean film air temperature.

The local Nusselt number (Nu_z) can be then determined as:

$$Nu_z = \frac{h_z \quad D_h}{k} \quad \ldots(9)$$

Where:

K=thermal conductivity of air = 0.6099 W/m^2°C

The average values of Nusselt number Nu_m can be calculated as follows:

$$Nu_m = \frac{1}{L}\int_o^L Nu_z\, dz \quad \ldots(10)$$

The average values of the other parameters can be calculated based on calculation of average cylinder surface temperature and average bulk air temperature as follows:

$$\overline{T_s} = \frac{1}{L}\int_{z=0}^{z=L} (T_s)_z \quad dz \quad \ldots(11)$$

$$\overline{T_b} = \frac{1}{L}\int_{z=0}^{z=L} (T_b)_z \quad dz \quad \ldots(12)$$

$$\overline{T_f} = \frac{\overline{T_S} + \overline{T_b}}{2} \quad \ldots(13)$$

$$Re_m = \frac{\rho \quad u_i \quad D_h}{\mu} \quad \ldots(14)$$

$$Gr_m = \frac{g \quad \beta \quad D_h^{\,3} \quad \left(\overline{T_s} - \overline{T_b}\right)}{\nu^2} \quad \ldots(15)$$

$$Pr_m = \frac{\mu \quad C_p}{k} \quad \ldots(16)$$

$$Ra_m = Gr_m\, Pr_m \quad \ldots(17)$$

Where;

$$\beta = 1/\left(273 + \overline{T_f}\right)$$

$$u_i = \dot{V}/A$$

$$A = \pi \quad \left(r_o^2 - r_i^2\right)$$

All the air physical properties ρ, μ, ν, and k were evaluated at the average mean film temperature ($\overline{T_f}$).

Results and Discussion

1. Temperature Variation

The variation of inner surface temperature of the outer cylinder along the axial distance for the same heat flux and Reynolds number, and for different Taylor number and exciting frequencies is plotted, for the selected runs, in Figs.(2-15).
In general, these figures show that the inner surface temperature of the outer cylinder decreases along the length of the cylinder with different values of frequencies if Reynolds number is kept constant, when the outer cylinder is under forced vibration in comparison to that without vibration.

This is attributed to the fact that the vibration of the outer cylinder affects on the boundary layers adjacent to the inner surface of the outer cylinder. The increase of boundary layer thickness leads to improve the heat transfer process between the cited surface and the bulk temperature of the flowing air. However, the designated effect depends on the response of the vibrating outer cylinder. This can be clearly seen in the cited figures.

The effect of vibration on the surface cylinder temperature variation for q=468 W/m^2 and Reynolds numbers (514, 931, 1316, 1509 & 1991) and Taylor number ($10.44x10^4$ & $8223x10^4$) is shown in Figs.(2-5), respectively. These figures reveal a decreasing in surface temperature along the length of the cylinder as the annulus vibrated by the excitation frequency (32 & 77) Hz. However, this decreasing in surface temperature is relatively greater at the excitation frequency (32 Hz) rather than (77 Hz). This may be attributed to the decreasing in the values of the natural frequencies of the outer cylinder due to the heat added by the heat flux.

Figures (6-9) show the same behavior mentioned before in Figs.(2-5) with the increasing of heat flux to q=642 W/m^2. Figures (10 to 13) manifest the effect of frequency on the temperature distribution of the same parameters taken in Figs.(2 to 9) but at higher heat flux q=920 W/m^2. As be shown, the difference between the values of temperature with frequency Fr=32 Hz and without frequency at different values of Reynolds number and $Ta=10.44x10^4$, as shown in Fig.(10), is greater than other values of angular velocity of the inner cylinder and frequencies. This behavior can be explained as follows: increasing the heat flux may shift the natural frequencies to lower values, then the excitation frequency may become very near to the natural frequency, and hence a violent vibration will be expected. Increasing the vibration response is higher in the case of the low angular velocity of inner cylinder than that of high angular velocity. As a result, an improve in the heat transfer process will be attained, as shown in Fig.(10).

Figures (14 & 15) exhibit the influence of change of the value of the frequency on the outer cylinder surface temperature for Re=514 and $Ta=10.44x10^4$& $Ta=8223x10^4$, respectively with different heat fluxes. It is noticed that there is no change in the values of temperature upstream. Then, beyond X=0.2 m, the values of temperature decrease as the frequency value increases at the same values of heat flux, Reynolds number and Taylor number. Downstream, the values of temperature begin to converge with each other because the strong effect of the natural convection currents in the case of low frequencies which improve the heat transfer process. Similarly, if the Reynolds number values increase to 931, 1316, 1509 and 1991 with $Ta=10.44x10^4$ & $Ta=8223x10^4$, as shown in Figs.(16-23); respectively, the same behavior will be obtained. This may be attributed to the fact that increasing the

angular velocity of the inner cylinder may create air vortices around and along the outer wall of the inner cylinder, which intern improve the heat transfer process.

2. Local Nusselt Number (Nu_x)

The effect of heat flux (q=468, 642 & 920 W/m^2) and vibrated frequency (Fr=0, 32, 77 Hz) on the local Nusselt number (Nu_x) with a logarithmic dimensionless axial distance (inverse Graetz number $Gz^{-1} = \frac{x/D}{Pr\ Re}\ h$), is plotted at Re=514, 931, 1316 &1991 with Ta=10.44x10^4& Ta=8223x10^4 at each value of Reynolds number in Figs.(24 to 33), respectively. In general, it is noticed from these figures the following facts:

1. The local Nusselt number values increase with increasing of heat flux which its effect reduces as Reynolds number increases, and the values of local Nusselt number converge with each other. This may be ascribed to the secondary flow super imposed on the forced flow effect leading to the higher heat transfer coefficient.
2. The heat transfer process improves as the vibrated frequency increases, especially in the middle region rather that upstream and downstream. This improvement appears more pronounced at high Reynolds number.
3. At low Reynolds number and at any Taylor number and heat flux at the outer fixed cylinder, the value of local Nusselt number decreases with the axial distance of annulus to reach a point, then it begins to increase downstream. The distance from beginning of annular gap to this point is called the thermal length of boundary layer or the thermal entrance region. As Reynolds number increases, the deviation of decreasing of the local Nusselt number values reduces, and the local value of Nusselt becomes relatively constant at Re=1991 in thermal entrance region, as shown in Figs.(32 & 33).
4. There is no pronounced effect of vibration frequency downstream.

Figures (34-45) show the effect of Reynolds number and vibrated frequency on the local Nusselt number along the dimensionless axial distance at variable heat flux (q=468, 642 &920) with Ta=10.44x10^4& Ta=8223x10^4, respectively. As can be seen, the values of the local Nusselt number increase as Re increases at the same value of frequency, heat flux and Taylor number because the of dominant forced convection on the heat transfer process. The effect of vibrated frequency appears more pronounced in Fr=32 Hz than Fr=77 Hz at low heat flux q=468 W/m^2 as shown in Figs.(34-37) and relatively be equal at medium value of heat flux q=642 W/m^2 as shown in Figs.(38-41) and returns to be larger in Fr=32 Hz than Fr=77 Hz at high value of heat flux q=920 W/m^2, as shown in Figs.(42-45).

It is obvious also for constant heat flux that the deviation of Nu_x value moves towards the left and increases as the Reynolds number increases due to a decrease in the inverse Greatz number (Gz^{-1}). This behavior of the local Nusselt number focused the light on the dominating forced convection on the heat transfer process.

3. Effect of Excitation Frequency on Temperature Differences

Figures (46 & 47) exhibit the average temperature differences along the inner surface of the outer cylinder versus different heat flux (q). As it can be seen, the temperature differences decreases with the increase of excitation frequency of vibrations from (32 to 77) Hz at the same applied heat flux. On the other hand, the

reduction in the temperature difference enhanced the performance of the heat transfer process along the outer cylinder of annulus. In all cases, the temperature differences increases approximately linearly with the increase of the heat flux at the same frequency.

Figures (48 & 49) show the temperature difference of the average outer cylinder wall with and without vibration against the heat flux along the outer wall of annulus at Re=1316 and Ta=$10.44x10^4$& Ta=$8223x10^4$, respectively. It is obvious that the relation between the temperature difference and the heat flux changes from linear at Re=514 to non-linear (quadratic) at Re=1316, but the general behavior is the same. In addition, the average temperature difference for low value of Re is larger than that at high Re.

Besides the large accelerations and decelerations to which the heat transfer surface is subjected during the vibration, there appear to be other factors which decide whether the surface carries the boundary layer with it or vibrates in an enclosed fluid film. Indeed, the nature of the phenomenon associated with the vibration of the heat transfer surface is so complicated that a simple correlation or analysis of the mechanism cannot be achieved.

4.Average Nusselt Number

The values of the average Nusselt number (Nu_m) for vertical annulus with rotating inner cylinder are plotted in Figs.(50 and 51); respectively, in the form of log(Nu_m) against log(Ra/Re) for the values of Ta are $10.44x10^4$& $8223x10^4$. The Reynolds number values vary from 514 to 1991, and Ra from 9.378×10^4 to 1.9044×10^5. All the points as can be seen are represented by linearization of the following equations:

Without vibration $$Nu_m=1.5304\ Re^{0.5632}\times Ta^{-0.2816}\times Ra^{0.2816} \quad ...(18)$$

With vibration $$Nu_m=1.7725\ Re^{0.4612}\times Ta^{-0.2308}\times Ra^{0.2308}\times Fr^{0.2308} \quad ...(19)$$

It is shown that the heat transfer equations have the same following form:

$$Nu_m=C_1\ Re^A\ Ta^B\ Ra^D \quad \ldots(20)$$

$$Nu_m=C_2\ Re^E\ Ta^F\ Ra^H\ Fr^L \quad \ldots(21)$$

The values of measured Nu_m are compared with that of Nu_m calculated from Eq.(19) for aiding flow as shown in Fig.(52). This figure shows the range of deviation equals to ±21%.

5.Comparison with Previous Experimental Work

The local Nusselt number variations with the dimensionless axial distance for the present experimental work (Re^2/Ta=0.2, Re=514, q=100 W/m^2) is compared with that of the experimental work of [15] (Re^2/Ta=0.2, Re=500, q=100 W/m^2) as shown in Fig.(53). It is obvious that the behavior and trend of Nu_x with (Gz^{-1}) for the two works are the same with a maximum difference 19.6%, minimum difference 8.5%, and mean difference 14.05%. The difference between the two experimental works may be referred to the experimental errors and the difference in the values of ratio L/D_h between them.

Conclusions

1- The rate of heat transfer enhances by using forced vibration to the system.

2- The variation of the inner surface temperature along the axial axis without vibration of outer cylinder has the same trend as annulus with vibration.

3- The Nu_x is affected by many variables summarized in the following points:

a. For the same Re, Ta and Fr, the Nu_x increases with increasing of heat flux.

b. For the same heat flux and frequency, the Nu_x increases with increasing the rotational velocity of inner cylinder (i.e., Tayler number).

c. For the same Re, Ta and heat flux, the Nu_x increases with increasing the amplitude of the cylinder at excitation frequency.

4. An empirical equation for the average Nusselt number as a function of Reynolds number, Rayliegh number, Taylor number and frequency has been deduced.

Nomenclature:

SYMBOL	DESCRIPTION	UNITS
A_i	Cross section of element (i)	m^2
A1	Outer surface area of inner cylinder	m^2
b	Gap width (r_2-r_1)	m
C_p	Specific heat at constant pressure	kJ/kg.K
D_h	$2(r_2-r_1)$	m
Fr	Frequency	Hz
g	Gravity acceleration	m/s^2
h	Heat transfer coefficient	$W/m^2.K$
I	Current	Amp.
L	Length of cylinder	m
$\dot{m}$	Mass flow rate	kg/s
Nr	Radius ratio	r_1/r_2
p	Pressure	N/m^2
Q	Total heat power	W
q	Heat flux	W/m^2
r	Radial coordinate	m
r_1	Outer radius of inner cylinder	m
r_2	Inner radius of outer cylinder	m
t	Temperature	^oC
u	Axial velocity	m/s
v	Radial velocity	m/s
V”	Voltage	volt
w	Tangential velocity	m/s
z	Axial coordinate	m

Creak Symbols

SYMBOL	DESCRIPTION	UNITS
α	Thermal diffusivity	m^2/s
β	Coefficient of volume expansion	1/K
μ	Dynamic viscosity	Kg/m.s
ν	Kinematic viscosity	m^2/s
ρ	Density	kg/m^3
ρ_i	Density at entrance	kg/m^3
ω	Angular velocity of inner cylinder	rad./s
κ	Thermal conductivity	W/m K
Δ	Difference between two values	–

Dimensionless Group

SYMBOL	DESCRIPTION	EQUATION
A	Aspect ratio	$r_2–r_1/r_1$
Gr	Grashof number	$gbqr_1^4 \Big/ kn^2$
Nu	Nusselt number	$h.D_h/\kappa$
Pr	Prandtl number	$\mu.Cp/\kappa$
R	Radial coordinate	r/r_2
Ra	Rayligh number	Gr.Pr
Re	Reynolds number	$u_i.D_h/\upsilon$
Ri	Richardson number	Gr/Re^2
RR	Radial coordinate	$r–r_1/r_2–r_1$
Ta	Taylor number	$2\eta^2.r_1^2.b^3/\upsilon^2(r_1+r_2)$
Gz^{-1}	Inverse Graetz number	$z/Re.Pr.D_h$

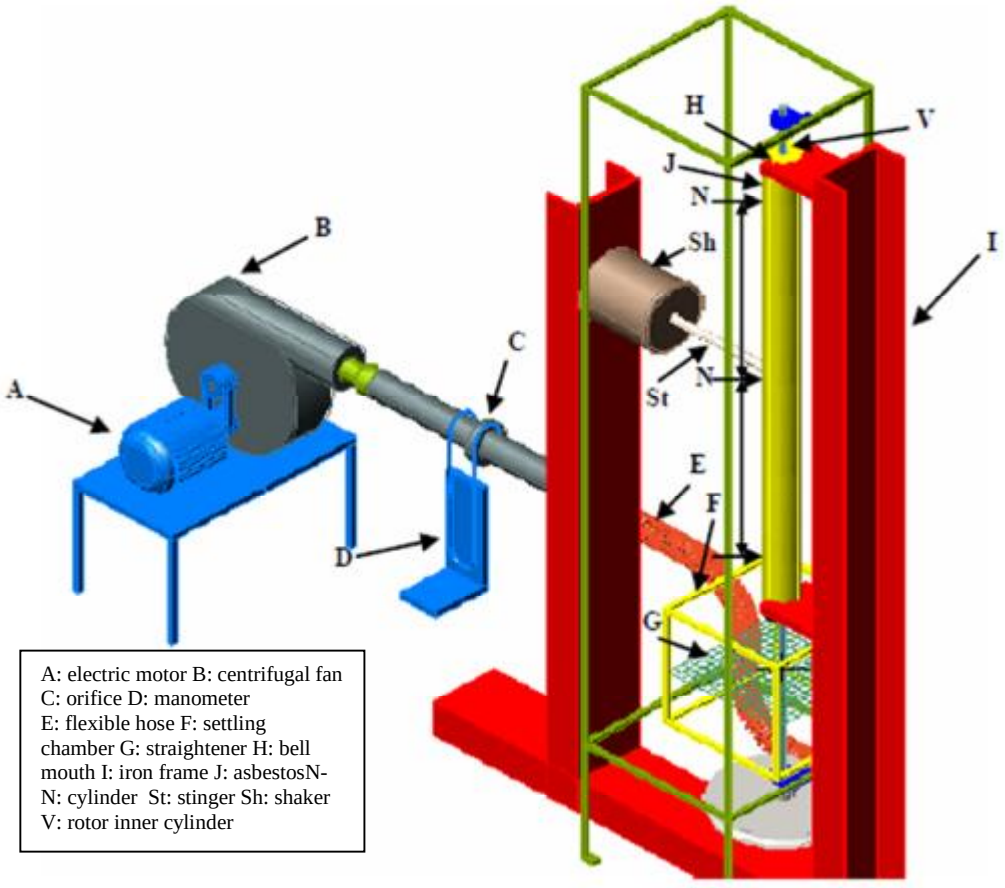

Figure.(1) Schematic Diagram of Experimental Apparatus

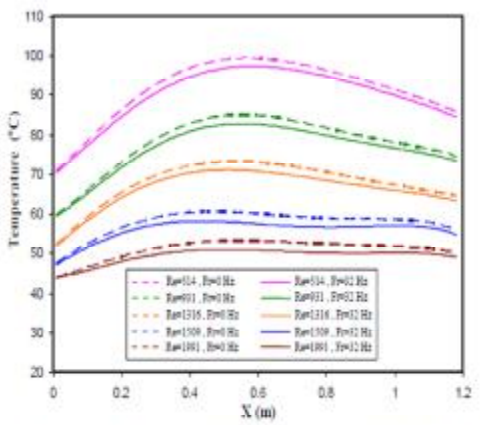

Fig.(2): Variation of the Surface Temperature with the Axial Distance at q=468W/m^2, Ta=10.44×10^4, Fr=32 Hz

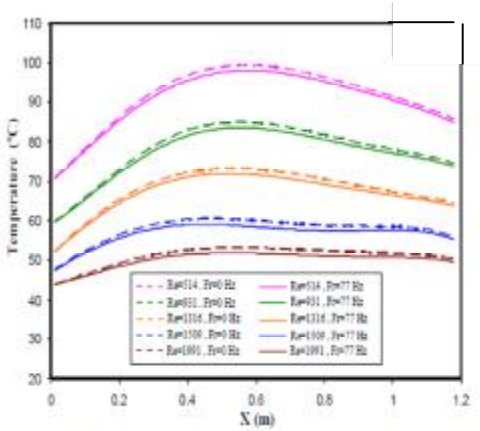

Fig.(3): Variation of the Surface Temperature with the Axial Distance at q=468W/m^2, Ta=10.44×10^4, Fr=77 Hz

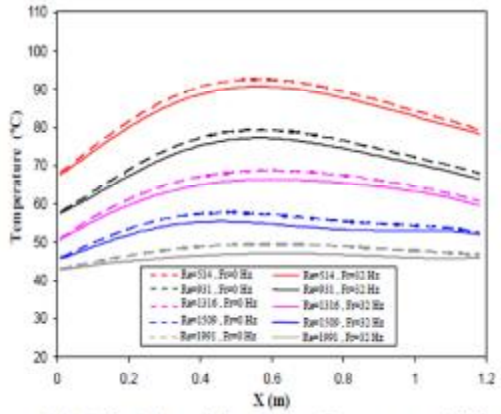

Fig.(4): Variation of the Surface Temperature with the Axial Distance at q=468W/m^2, Ta=82.23×10^4, Fr=32 Hz

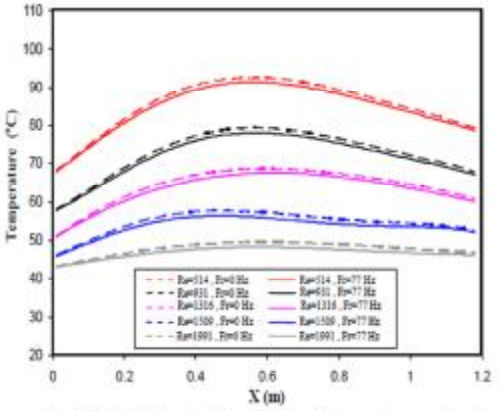

Fig.(5): Variation of the Surface Temperature with the Axial Distance at q=468W/m^2, Ta=82.23×10^4, Fr=77 Hz

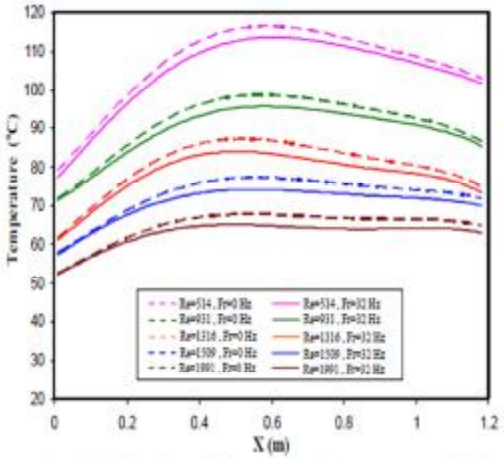

Fig.(6): Variation of the Surface Temperature with the Axial Distance at q=642W/m^2, Ta=10.44×10^4, Fr=32 Hz

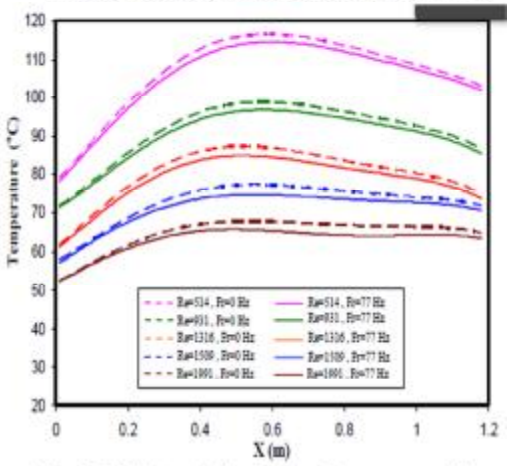

Fig.(7): Variation of the Surface Temperature with Axial Distance at q=642W/m^2, Ta=10.44×10^4, Fr=77 Hz

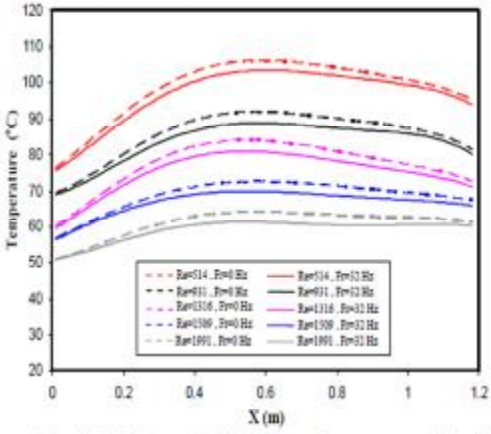

Fig.(8): Variation of the Surface Temperature with the Axial Distance at q=642W/m^2, Ta=82.23×10^4, Fr=32 Hz

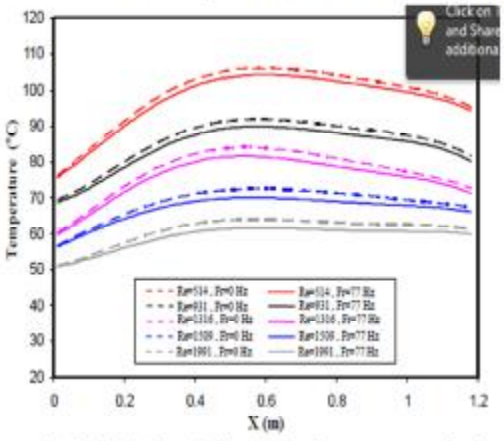

Fig.(9): Variation of the Surface Temperature with the Axial Distance at q=642W/m^2, Ta=82.23×10^4, Fr=77 Hz

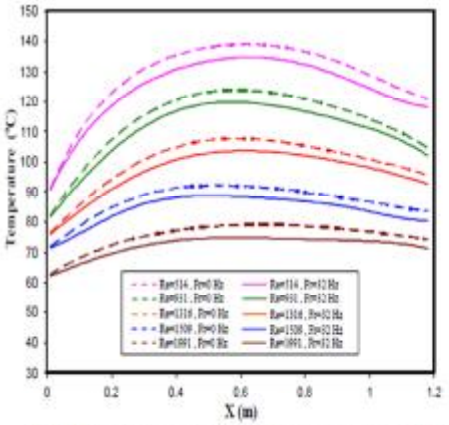

Fig.(10): Variation of the Surface Temperature with the Axial Distance at q=920W/m^2, Ta=10.44×10^4, Fr=32 Hz

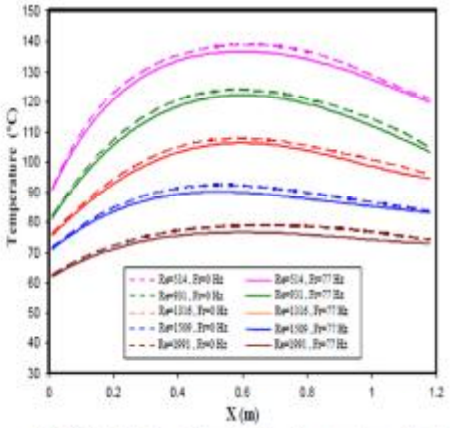

Fig.(11): Variation of the Surface Temperature with the Axial Distance at q=920W/m^2, Ta=10.44×10^4, Fr=77 Hz

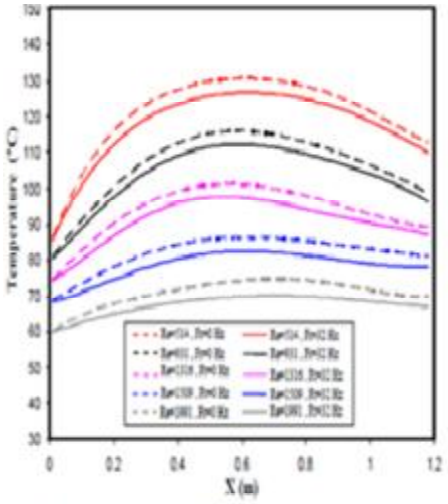

Fig.(12): Variation of the Surface Temperature with the Axial Distance at q=920W/m^2, Ta=82.23×10^4, Fr=32 Hz

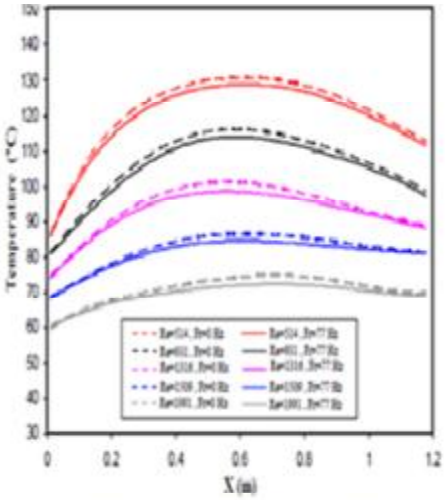

Fig(13) Variation of the Surface Temperature Axial Distance at q=920W/m^2, Ta=82.23×10^4, Fr=77 Hz

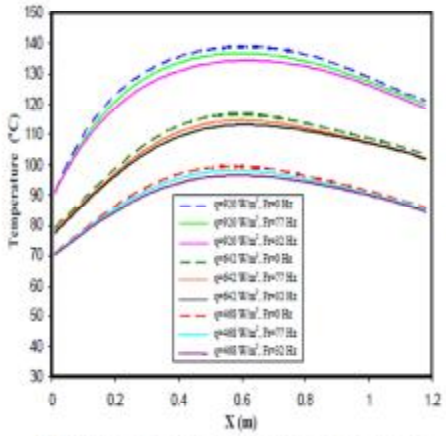

Fig.(14): Variation of the Surface Temperature with the Axial Distance at Re=514 & Ta=10.44×10^4

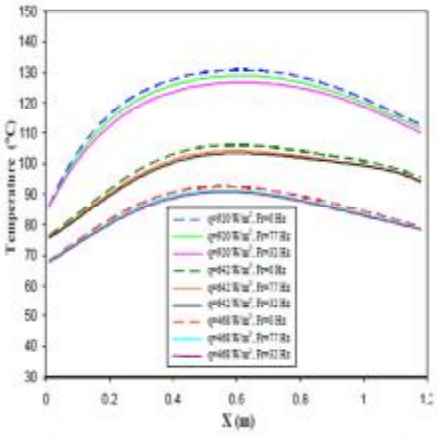

Fig.(15): Variation of the Surface Temperature with the Axial Distance at Re=514 & Ta=82.23×10^4

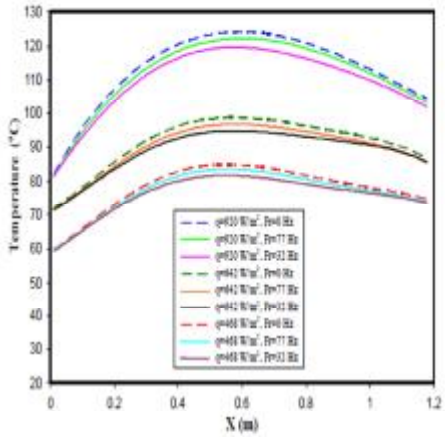

Fig.(16): Variation of the Surface Temperature with the Axial Distance at Re=931 & Ta=10.44×10^4

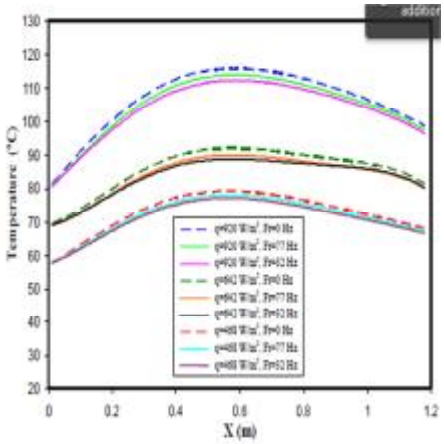

Fig.(17): Variation of the Surface Temperature with the Axial Distance at Re=931 & Ta=82.23×10^4

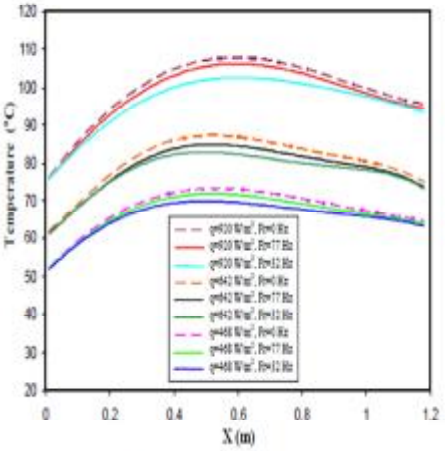

Fig.(18): Variation of the Surface Temperature with the Axial Distance at Re=1316 & Ta=10.44×10^4

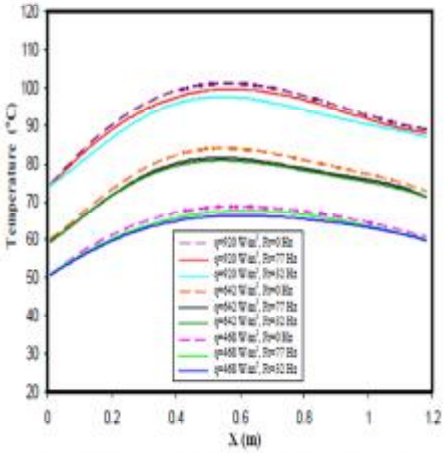

Fig.(19): Variation of the Surface Temperature with the Axial Distance at Re=1316 & Ta=82.23×10^4

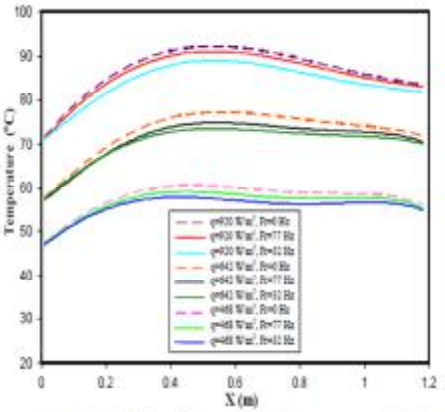

Fig.(20): Variation of the Surface Temperature with the Axial Distance at Re=1509 & Ta=10.44×10^4

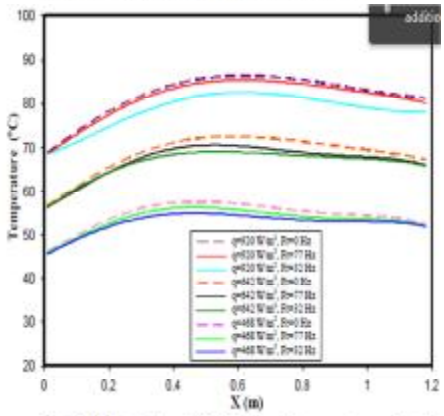

Fig.(21): Variation of the Surface Temperature with the Axial Distance at Re=1509 & Ta=82.23×10^4

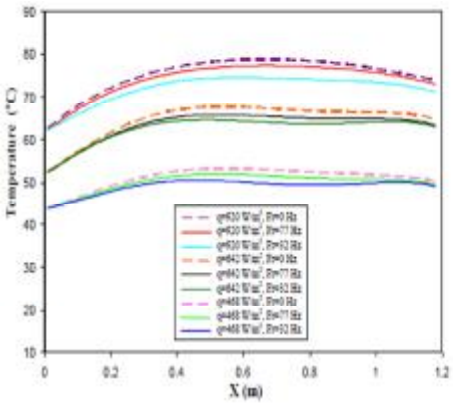

Fig.(22): Variation of the Surface Temperature with the Axial Distance at Re=1991 & Ta=10.44×10^4

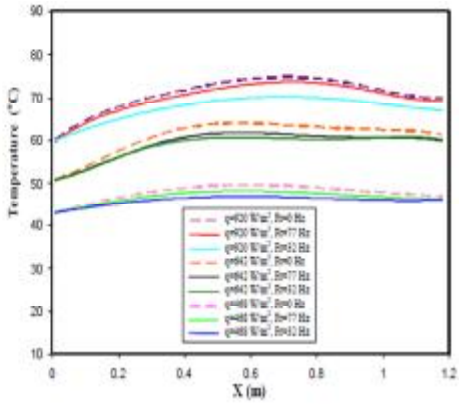

Fig.(23): Variation of the Surface Temperature with the Axial Distance at Re=1991 & Ta=82.23×10^4

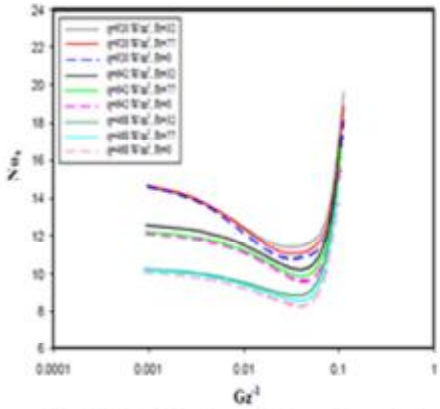

Fig.(24): Local Nusselt number Versus Dimensionless Axial Distance at Re=514 & Ta=10.44×10^4

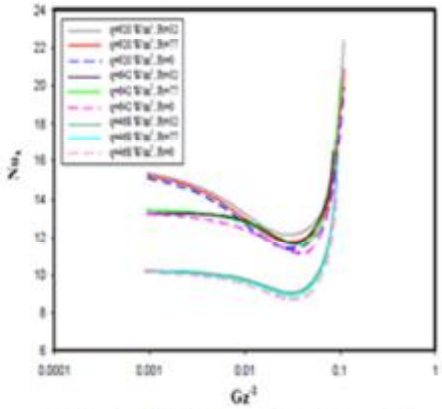

Fig(25) Local Nusselt number Versus Dimensionless Axial Distance at Re=514 & Ta=82.23×10^4

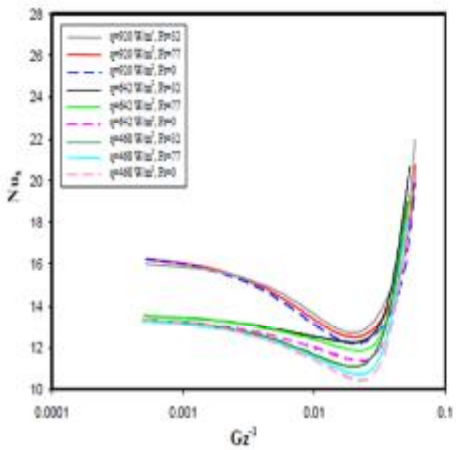

Fig.(26): Local Nusselt number Versus Dimensionless Axial Distance at Re=931 & Ta=10.44×10^4

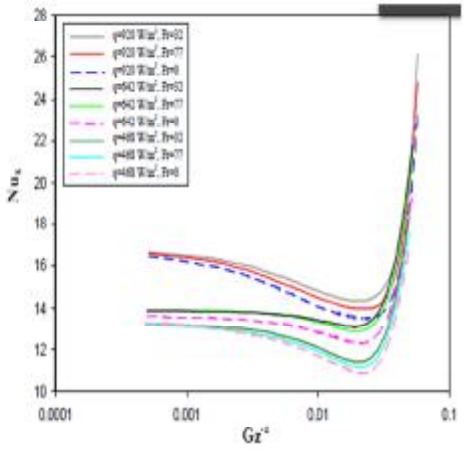

Fig.(27): Local Nusselt number Versus Dimensionless Axial Distance at Re=931 & Ta=82.23×10^4

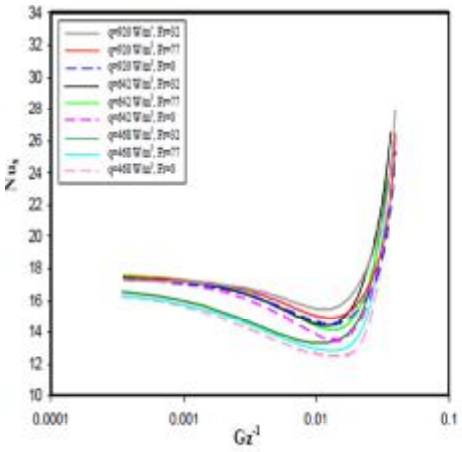

Fig.(28): Local Nusselt number Versus Dimensionless Axial Distance at Re=1316 & Ta=10.44×10^4

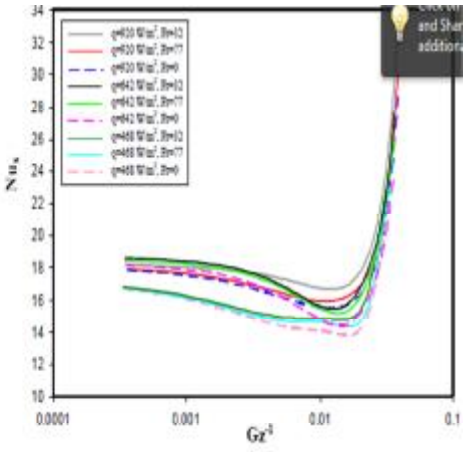

Fig.(29): Local Nusselt number Versus Dimensionless Axial Distance at Re=1316 & Ta=82.23×10^4

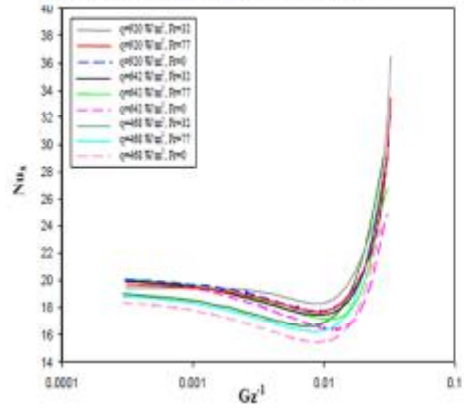

Fig.(30): Local Nusselt number Versus Dimensionless Axial Distance at Re=1509 & Ta=10.44×10^4

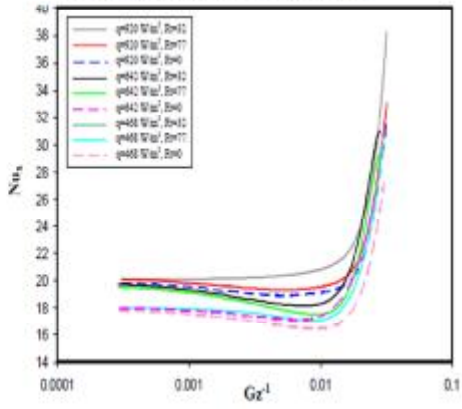

Fig.(31): Local Nusselt number Versus Dimensionless Axial Distance at Re=1509 & Ta=82.23×10^4

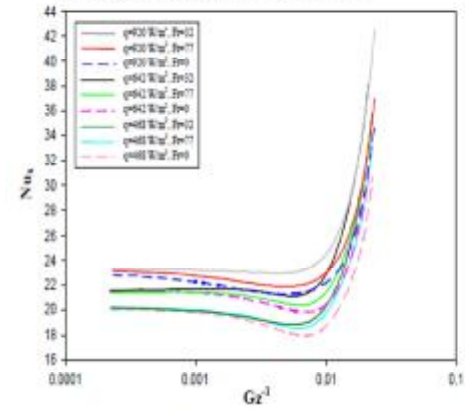

Fig.(32): Local Nusselt number Versus Dimensionless Axial Distance at Re=1991 & Ta=10.44×10^4

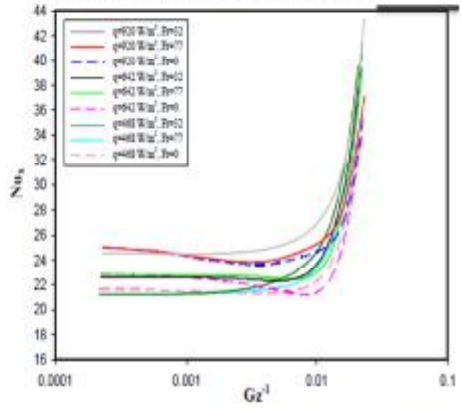

Fig.(33): Local Nusselt number Versus Dimensionless Axial Distance at Re=1991 & Ta=82.23×10^4

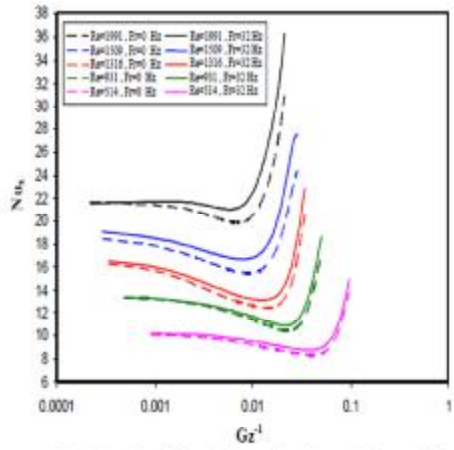

Fig.(34): Local Nusselt number Versus Dimensionless Axial Distance at q=468W/m^2, Ta=10.44×10^4, Fr=32 Hz

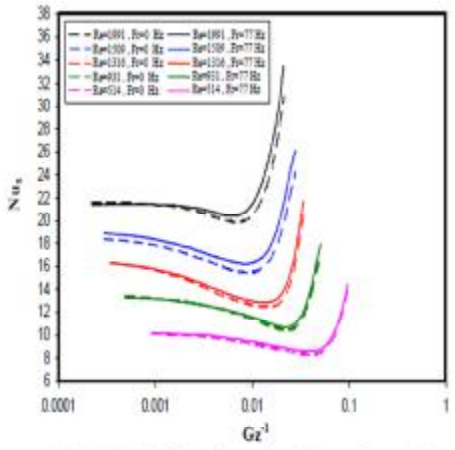

Fig.(35): Local Nusselt number Versus Dimensionless Axial Distance at q=468W/m^2, Ta=10.44×10^4, Fr=77 Hz

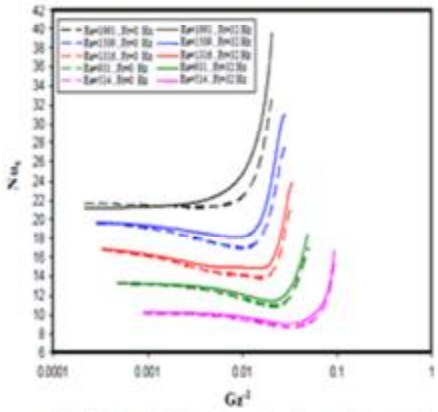

Fig.(36): Local Nusselt number Versus Dimensionless Axial Distance at q=468W/m^2, Ta=82.23×10^4, Fr=32 Hz

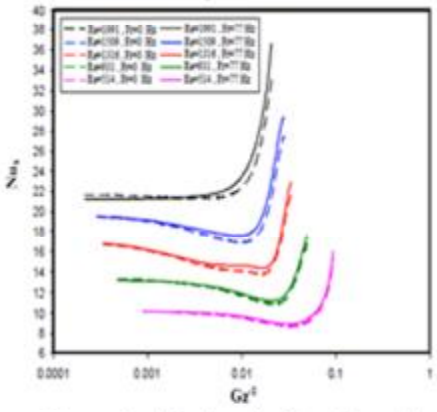

Fig(37) Local Nusselt number Versus Dimensionless Axial Distance at q=468W/m^2, Ta=82.23×10^4, Fr=77 Hz

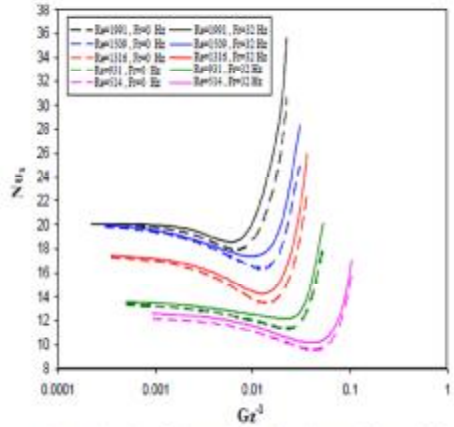

Fig.(38): Local Nusselt number Versus Dimensionless Axial Distance at q=642W/m^2, Ta=10.44×10^4, Fr=32 Hz

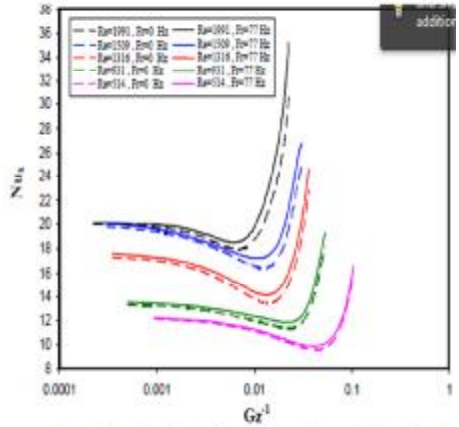

Fig.(39): Local Nusselt number Versus Dimensionless Axial Distance at q=642W/m^2, Ta=10.44×10^4, Fr=77 Hz

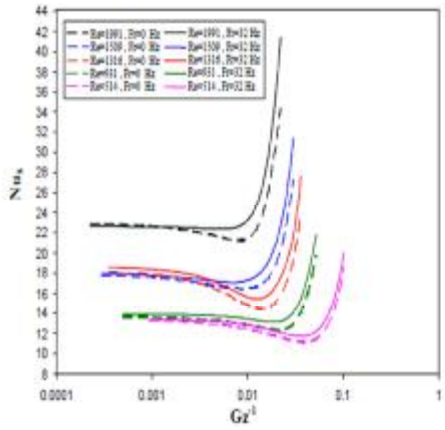

Fig.(40): Local Nusselt number Versus Dimensionless Axial Distance at q=642W/m^2, Ta=82.23×10^4, Fr=32 Hz

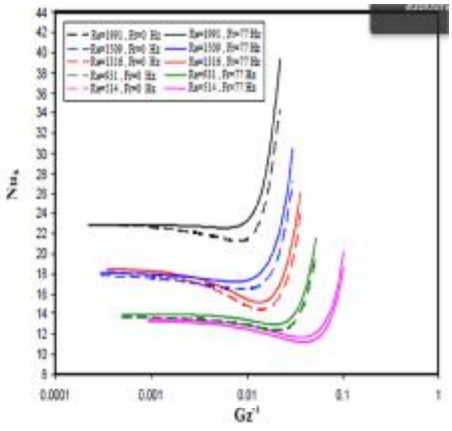

Fig.(41): Local Nusselt number Versus Dimensionless Axial Distance at q=642W/m^2, Ta=82.23×10^4, Fr=77 Hz

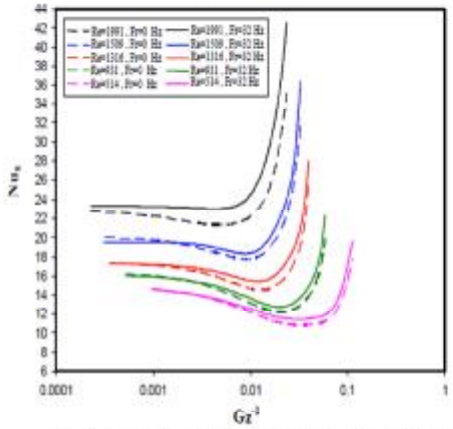

Fig.(42): Local Nusselt number Versus Dimensionless Axial Distance at q=920W/m^2, Ta=10.44×10^4, Fr=32 Hz

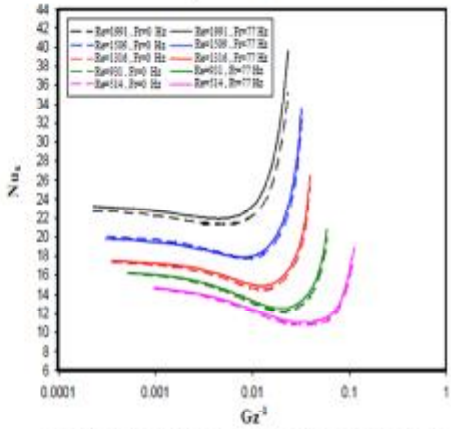

Fig.(43): Local Nusselt number Versus Dimensionless Axial Distance at q=920W/m^2, Ta=10.44×10^4, Fr=77 Hz

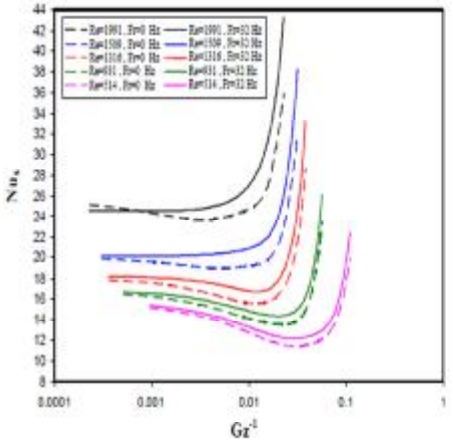

Fig.(44): Local Nusselt number Versus Dimensionless Axial Distance at q=920W/m^2, Ta=82.23×10^4, Fr=32 Hz

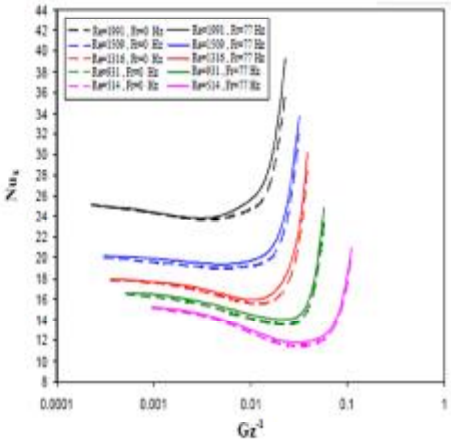

Fig.(45): Local Nusselt number Versus Dimensionless Axial Distance at q=920W/m^2, Ta=82.23×10^4, Fr=77 Hz

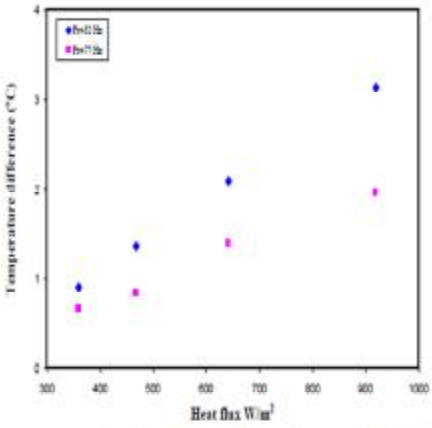

Fig.(46): Change in temperature difference between with and without vibration of the frequency vibrations at Re=514 & Ta=10.44×10⁴

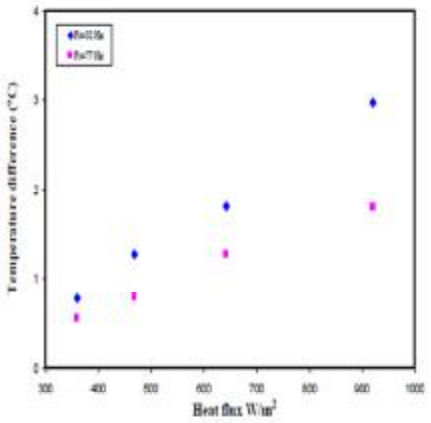

Fig.(47): Change in temperature difference between with and without vibration of the frequency vibrations at Re=514 & Ta=82.23×10⁴

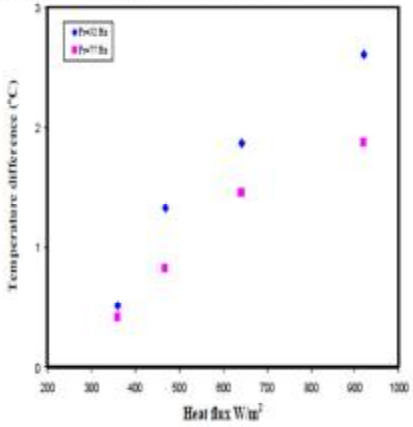

Fig.(48): Change in temperature difference between with and without vibration of the frequency vibrations at Re=1316 & Ta=10.44×10⁴

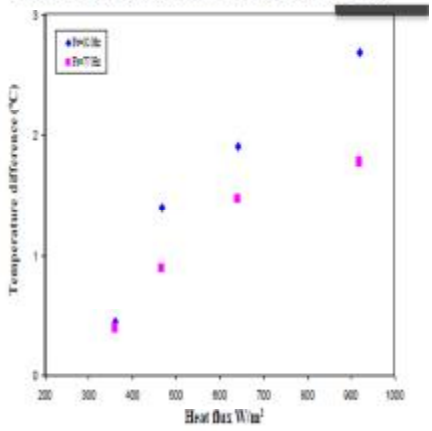

Fig.(49): Change in temperature difference between with and without vibration of the frequency vibrations at Re=1316 & Ta=82.23×10⁴

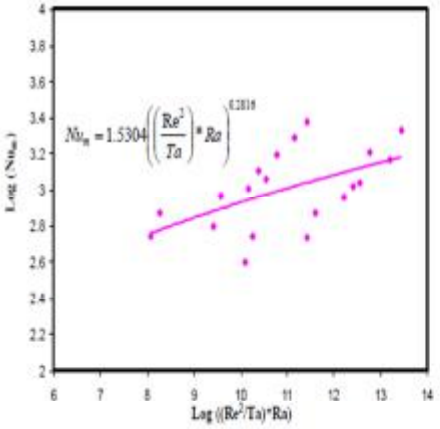

Fig.(50): Experimental Average Nusselt number Versus ((Re²/Ta)*Ra)

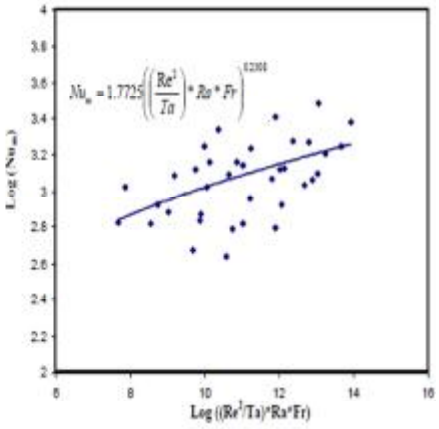

Fig.(51): Experimental Average Nusselt number Versus ((Re²/Ta)*Ra*Fr)

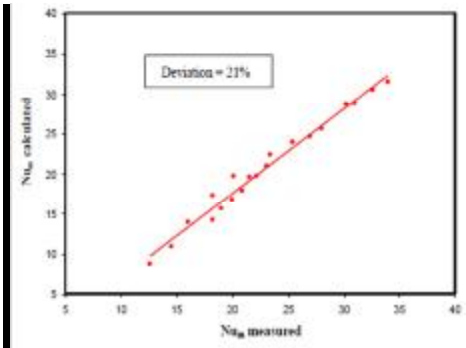

Fig.(52) Comparison Between Measured Nu_m and Nu_m Calculated from Eq.(19)

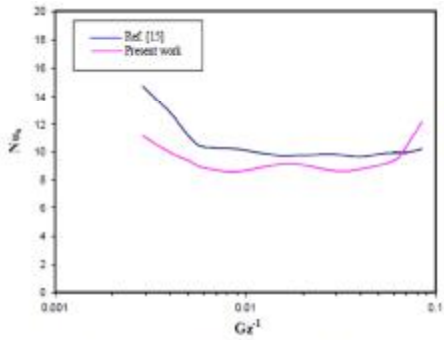

Fig.(53): Comparison of the Present Experimental Work with the Work of Ref. [15]

References

[1] A . M . Rishem, "Numerical Study of the Effect of Horizontal Vibration on Forced Convection Heat Transfer from a Vertical Cylinder ", M . Sc. Thesis, Mechanical Engineering Dept., University of Baghdad, 2005.

[2] K. Hashimoto, N. Akino, and H. Kawamura, "Combined Forced- Free Convection Heat Transfer to a Highly Heated Gas in a Vertical Annulus" , Int. J. Heat Mass Transfer, Vol.29 , pp. 145-151, 1986.

[3] R .Anantanarayanan and A .Ramachandran, "Effect of Vibration on Heat Transfer from a Wire to Air in Parallel Flow", Trans. Amer.Soc. Mech. Engr.,Vol.80, pp.1426-1432, 1958.

[4] R. Lemlich, "A Musical Heat Exchanger", Journal of heat transfer Trans. ASME. Vol.83, pp.385-386, 1961.

[5] R. Lemlich, "Vibration and Pulsation Boost Heat Transfer", Chemical Engineering. Vol 68, pp. 171-176, 1961.

[6] K. Seenivasan and A. Ramachandran, "Effect of on Heat Transfer from a Horizontal Cylinder to a Normal Air Stream, "Int. J. Heat and Mass Transfer, Vol.3, pp.60-67, 1961.

[7] B. H. Thrasher, "Oscillatory Heat Transfer", PhD Dissertation, University of Alabama, 1967.

[8] J. M. Faircloth and W. J. Schaaetzle, "Effect of Vibration on Heat Transfer for Flow Normal to a Cylinder" Trans. ASME. Journal of Heat Transfer, pp. 140-144, 1969.

[9] Susumu Kotake and Isao Aoki, "Heat Transfer of Cylinder in Large -Amplitude Oscillating Wake Flow", Int. J. Heat and Mass Transfer, Vol. 27, No. 10, pp. 1903-1917, 1984.

[10] Makki. H. Al-Ubaydi, "Study of Influence of Vertical Vibration on Heat Transfer Coefficient by Free Convection from Cylinders", M. Sc. Thesis, University of Technology, 2001.

[11] Yong Ho Lee and Soon Heung Chang, "The Effect of Vibration on Critical Heat Flux in a Vertical Round Tube, "J. Nuclear Science and Technology, Vol. 40, No. 10, pp. 734-743, 2003.

[12] Dae Hun Kim, Yong Ho Lee, and Soon Heung Chang, "Effects of Mechanical Vibration on Critical Heat Flux in Vertical Annulus Tube, "Nuclear Engineering and Design, 237, pp. 982–987, 2007.

[13] J. P. Holman, "Experimental Method for Engineers, "McGraw-Hill ,Tokyo, Japan, 4th Edition, 1984.

[14] J. Grimson, "Advance fluid dynamic and heat transfer, " Mc Graw-Hill, England, 1971.

[15] Akeel A. Mohammed, "An Investigation into Laminar Combined Convection Heat Transfer through Concentric Annuli", Ph.D. Thesis, Mechanical Engineering Dept., University of Technology, September, 2005.